ARTICLES

Journal of Semiconductors
(2022) 43, 112502
doi: 10.1088/1674-4926/43/11/112502

Colossal negative magnetoresistance from hopping in insulating ferromagnetic semiconductors

Xinyu Liu†, Logan Riney, Josue Guerra, William Powers, Jiashu Wang, Jacek K. Furdyna, and Badih A. Assaf

Department of Physics and Astronomy, University of Notre Dame, Notre Dame, IN 46556, USA

Abstract: Ferromagnetic semiconductor $Ga_{1-x}Mn_xAs_{1-y}P_y$ thin films go through a metal–insulator transition at low temperature where electrical conduction becomes driven by hopping of charge carriers. In this regime, we report a colossal negative magnetoresistance (CNMR) coexisting with a saturated magnetic moment, unlike in the traditional magnetic semiconductor $Ga_{1-x}Mn_xAs$. By analyzing the temperature dependence of the resistivity at fixed magnetic field, we demonstrate that the CNMR can be consistently described by the field dependence of the localization length, which relates to a field dependent mobility edge. This dependence is likely due to the random environment of Mn atoms in $Ga_{1-x}Mn_xAs_{1-y}P_y$ which causes a random spatial distribution of the mobility that is suppressed by an increasing magnetic field.

Key words: ferromagnetic semiconductor; colossal negative magnetoresistance; variable-range hopping; nearest-neighbor hopping; Anderson localization; spintronic

Citation: X Y Liu, L Riney, J Guerra, W Powers, J S Wang, J K Furdyna, and B A Assaf, Colossal negative magnetoresistance from hopping in insulating ferromagnetic semiconductors[J]. *J. Semicond.*, 2022, 43(11), 112502. https://doi.org/10.1088/1674-4926/43/11/112502

1. Introduction

Electronic transport studies of carrier localization provide a powerful tool for understanding doped disordered systems[1, 2]. At low temperatures, transport in such systems can occur through one of two processes. The first is the nearest-neighbor hopping (NNH), where a charge carrier hops from an occupied dopant impurity site to the nearest vacant impurity site. The second, referred to as variable-range hopping (VRH), occurs when there exists a path from an occupied dopant site to a vacant site at an optimum hopping distance that is further than the nearest unoccupied dopant site, but involves a lower energy barrier than the nearest unoccupied site[3]. That optimum distance is determined by a tradeoff between the spatial and energy penalties in the transition between the localized states involved[4]. The temperature dependence of the longitudinal resistivity in the hopping regime in the absence of interactions is described by the Mott VRH mechanism[5], with $\ln[\rho(T)] \sim (T_0/T)^{1/(d+1)}$, where d is the dimensionality of the system. Disorder-induced localization can reduce charge screening, making the Coulomb interaction between charge carriers important to consider. In this regime, the interplay between disorder and interactions makes the physics of electron transport more intriguing.

Efros and Shklovskii (ES)[6] noted that a soft energy gap will open at the Fermi level when long-range Coulomb interactions between charge carriers are included. The density of states at the Fermi level then vanishes, and the temperature dependence of the resistivity can be described by the so-called Efros-Shklovskii variable range hopping (ES-VRH) mechanism[7, 8], $\ln[\rho(T)] \sim (T_0/T)^{1/2}$, independent of dimensionality. Nearest neighbor hopping, variable range hopping, and related effects such as metal-insulator transitions, have been extensively discussed in many recent studies of disordered systems[9–13]. These observations have contributed significantly toward a better understanding of localized states at different energy levels within the band gap.

However, although it has been extensively studied in semiconductors with low doping, in insulating oxides[14] and in some glass-like systems[15], the physics of localization remains poorly understood in semiconductors exhibiting magnetic order. $Ga_{1-x}Mn_xAs$ has long been known to exhibit a metal–insulator transition driven by Mn doping, but only at doping concentrations that are sufficiently low to weaken the ferromagnetic exchange interaction[16]. Systems exhibiting an independent tuning of this transition and of the magnetic states are rare and generally limited to highly disordered and amorphous magnetic insulators. Our development of the magnetic semiconductors $Ga_{1-x}Mn_xAs_{1-y}P_y$ that can retain a ferromagnetic state across the metal-insulator transition enables studies of this physics in the presence of magnetism. In recent studies carried out on a series of ferromagnetic semiconductor $Ga_{1-x}Mn_xAs_{1-y}P_y$ alloys with high phosphorus content we have observed that the number of itinerant holes (*i.e.*, holes that contribute to the Hall effect) is significantly lower than the total hole concentration[17]. A large fraction of holes arising from Mn acceptors is thus localized at the acceptor sites. Such localization increases with increasing concentration of phosphorus y. As we vary the properties of $Ga_{1-x}Mn_xAs_{1-y}P_y$ from metallic to this semi-insulating regime by increasing the value of y, our studies of the anomalous Hall effect (AHE) in this material show a clear transition from AHE described by Berry curvature to one that is determined by hopping[18].

In this work, we show that the conductivity of magnetic semiconductors that approach the insulating regime but re-

Correspondence to: X Y Liu, Xinyu.Liu.30@nd.edu
Received 10 AUGUST 2022; Revised 8 SEPTEMBER 2022.

Table 1. Properties of $Ga_{1-x}Mn_xAs_{0.79}P_{0.21}$ films.

$Ga_{1-x}Mn_xAs_{1-y}P_y$	x	y	Curie temperature (K)	Magnetization (emu/cm^3)	Thickness (nm)
S1	0.06	0.21	40	23.9	47.2
S2	0.04	0.21	28	13.1	62.5

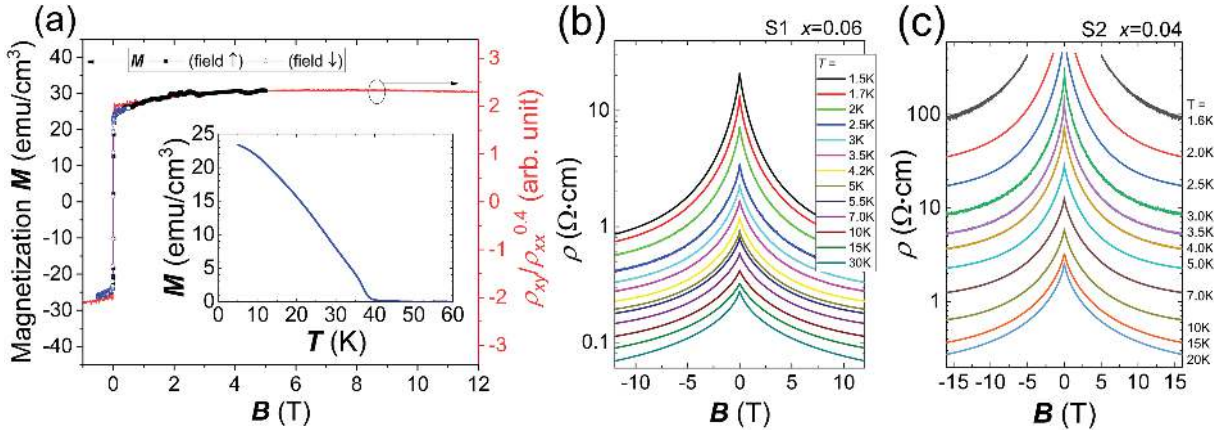

Fig. 1. (Color online) (a) Magnetization versus magnetic field measured at $T = 5$ K with magnetic field applied along the out-of-plane direction in $Ga_{0.94}Mn_{0.06}As_{0.79}P_{0.21}$. $\rho_{xy}/\rho_{xx}^{0.4}$ at 5 K is also plotted for comparison. Inset: Temperature dependence of magnetization measured along the out-of-plane [001] axis at $B = 2$ mT. (b) Resistivity of S1 ($Ga_{0.94}Mn_{0.06}As_{0.79}P_{0.21}$) and (c) that of S2 ($Ga_{0.94}Mn_{0.04}As_{0.79}P_{0.21}$) at several temperatures with magnetic field applied along the [001] axis.

main ferromagnetic show a crossover between NNH and VRH conduction that is driven by magnetic field. A colossal negative magnetoresistance develops through this crossover, driven by the changing localization length. Our analysis employs the temperature dependence of conductivity which we show follows the NNH regime at zero magnetic field and the ES-VRH scaling law at high magnetic field[6]. At low temperature, we show that the changing conductivity versus temperature at a fixed magnetic field yields a field dependent localization length ξ_{loc}, which drives the colossal magnetoresistance. The field dependence of ξ_{loc} suggests that magnetic randomness likely limits conductivity at very low temperatures in ferromagnetic semiconductors.

2. Experimental details

Two $Ga_{1-x}Mn_xAs_{1-y}P_y$ films used for this study were grown on GaAs (100) semi-insulating substrates by low temperature molecular beam epitaxy (MBE)[19, 20]. The Mn content x of the two films is 0.06 and 0.04; while the phosphorous mole fraction y is 0.21 in both films. In what follows we will refer to the two specimens as S1 and S2, respectively. Manganese and phosphorus concentrations, film thicknesses, Curie temperatures, and saturation magnetizations of specimens were determined by high resolution X-ray diffraction and SQUID magnetometry using a quantum design MPMS XL system[20]. Table 1 summarizes the Mn and P concentrations, thicknesses, magnetizations, and Curie temperatures of the two $Ga_{1-x}Mn_xAs_{1-y}P_y$ films. Six-point Hall measurements were used for measuring the longitudinal and transverse resistivities of the films, with the long dimension (the current direction) along the [110] orientation of the GaAs substrate. Measurements of longitudinal and Hall resistivities were performed as a function of magnetic field B applied perpendicular to the sample plane and temperature T. We carried out magnetotransport measurements in magnetic fields up to 16 T and at temperatures between 1.5 K and the Curie point.

3. Results and analysis

Temperature dependence of magnetization was measured with magnetic field applied perpendicular to the film plane (*i.e.*, along the [001] axis), showing Curie temperatures of films S2 and S1 as 28 and 40 K, respectively. Hysteresis loops of the two films measured at $T = 5$ K are shown in Fig. S1 in Supplementary Materials. Magnetization measurements performed up to 5 T shown in Fig. 1(a) on sample S1 confirm that at 5 K all Mn spins, including those involved in ferromagnetic and superparamagnetic orders[21], are fully saturated at fields above 2 T. The magnetization remains finite and large at zero magnetic field, confirming that the easy axis of the sample is perpendicular to its plane.

Prior to transport measurements, the samples were zero-field-cooled to the desired temperature. Fig. 1(a) shows $\rho_{xy}/\rho_{xx}^{0.4}$ versus magnetic field up to 12 T. It is noted that in the "hopping" regime ($\rho_{xx} > 0.1$ Ω·cm), which corresponds to properties of insulating ferromagnetic semiconductors[18, 22], the dependence of ρ_{xy} on ρ_{xx} can be described experimentally by the universal relation $\rho_{xy} \propto \rho_{xx}^{0.4} M$. The curve $\rho_{xy}/\rho_{xx}^{0.4}$ thus reproduces the behavior of the magnetization, demonstrating that the anomalous Hall effect is dominated by hopping contribution[18, 22]. This is expected, given that the resistivity of these two samples reaches the high values of 40 Ω·cm for sample S1 and more than 5000 Ω·cm for S2 at $T < 1.5$ K. Figs. 1(b) and 1(c) shows the colossal change in resistance observed at low temperatures for the two samples in question. At 1.5 K and up to 30 K, the resistivity changes by more than an order of magnitude for sample S1. This colossal change is sustained up to 7 K in S2. Increasing temperature weakens the magnetoresistance significantly (see Fig. S2(a) in Supplementary Materials) and reduces the resistivity. Such colossal negative magnetoresistance (CNMR) is often observed in disordered ferromagnets, in which it is most pronounced in the vicinity of T_C[23, 24]. In such case CNMR is often attributed to

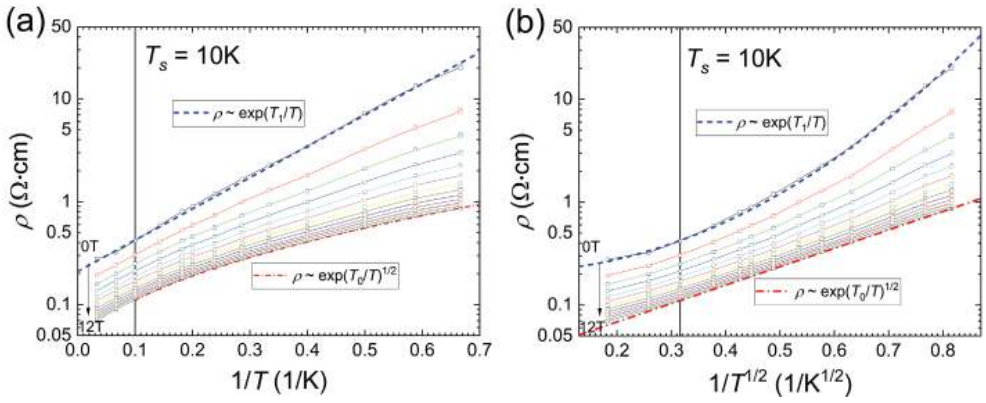

Fig. 2. (Color online) Resistivity of $Ga_{0.94}Mn_{0.06}As_{0.79}P_{0.21}$ sample with magnetic field applied along the [001] axis. (a) Scaling of resistivity versus $1/T$ at different magnetic fields. (b) Scaling of resistivity versus $T^{-1/2}$ at different magnetic fields.

electron scattering by fluctuating spins: The magnetic field increases the effective field acting on the localized spins and suppresses the fluctuation of spins at phase transition, which leads to the decrease of the resistivity. CNMR was also studied at low temperature in semi-insulating magnetic semiconductors with a low Curie temperature, but the mechanism is not fully understood[25, 26].

The remainder of this manuscript elucidates the relation of the CNMR with hopping transport mechanisms in $Ga_{1-x}Mn_xAs_{1-y}P_y$ where it coexists with a fully formed ferromagnetic state. To carry this out, we study the temperature dependence of the resistivity at different magnetic fields. Fig. 2(a) presents a semilogarithmic plot of longitudinal resistivity $\rho(B, T)$ as a function of inverse temperature for temperatures smaller than 10 K, measured on sample S1 at various fields B. As discussed in the literature[27–29], there are two basic hopping conduction processes that we must now consider: nearest-neighbor hopping (NNH) and variable-range hopping (VRH). In the NNH regime, it has been shown that the conductivity has the following temperature dependence[30]

$$\rho = \rho_1 \exp\left(\frac{W_{\mathrm{NNH}}}{k_{\mathrm{B}}T}\right) = \rho_1 \exp\left(\frac{T_1}{T}\right), \tag{1}$$

here $W_{\mathrm{NNH}} = k_{\mathrm{B}}T_1$ is an energy separation between the localized nearest-neighbor states. In the NNH conduction regime, an electron (or in our case a hole) with an activation energy of W_{NNH} hops to the nearest empty site. Note that this activation is generally much smaller than the energy required for thermally activated band conduction[31]. As shown in Fig. 2(a), although the temperature dependence of ρ is consistent with the NNH mechanism (dashed blue line) at 0 T, it deviates significantly from this behavior when a magnetic field is applied. Similar data for sample S2 are shown in Supplementary Materials. Thus, we conclude that a different mechanism must occur at low temperatures.

The density of delocalized carriers for samples S1 and S2 was estimated from their Curie temperatures as 3.8×10^{19} and 2.4×10^{19} cm^{-3}, respectively in an earlier publication[17]. These parameters lead to mobilities of 5.2×10^{-6} and 4.1×10^{-3} $cm^2/(V{\cdot}s)$, respectively. These are extremely low values compared to conventional semiconductors and metals, indicating strong carrier localization, consistent with Mott's hopping model[32]. The conductivity based on Mott hopping is given by[33]

$$\rho = \rho_0 \exp\left(\frac{T_0}{T}\right)^s, \tag{2}$$

where ρ_0 is a pre-exponential factor related to the resistivity at high temperatures, T_0 is a characteristic temperature that is inversely proportional to the localization length and $s = 1/4$ in the absence of interactions, and $s = 1/2$ is the presence of a Coulomb gap[6]. The latter comes from the ES-VRH model.

In Fig. 2(b), we plot the temperature dependence of $\ln(\rho)$ versus $1/T^{1/2}$. From that figure it is evident that the resistivity follows the ES-VRH model at high magnetic field, but violates it at low field, below 7 T. We thus conclude the following about the transport regimes present in our sample. At B = 0 T, transport is dominated by the NNH mechanism. Between 1 and 7 T, NNH and ES-VRH likely coexist. And above 7 T, the ES-VRH mechanism is dominant.

The data plotted in Fig. 2 is replotted in Fig. 3(a) and is shown along with a fit that takes into account the field-dependent crossover between NNH and VRH. To resolve the issue that no single conduction law satisfies the entire conductivity curve at any magnetic field, we can express Eq. (2) as[18, 34]:

$$\rho = \rho_0 T^{\alpha} \exp\left(\frac{T_0}{T}\right)^{1/2}. \tag{3}$$

Here T_0 has the same meaning as before, $1/T_0$ should be proportional to the localization length, T^{α} empirically accounts for non-VRH contributions at low fields, and α is a nonuniversal empirical constant that accounts for those contributions. The results of fitting to Eq. (3) for Sample S1 are shown in Figs. 3(b)–3(d), and for S2 in the Supplementary Materials .

As shown in Figs. 3(b) and 3(c), respectively, ρ_0 increases with magnetic field, and parameter α exponentially decays as a function of magnetic field, indicating that non-ES-VRH conduction (*i.e.*, NNH conduction) diminishes as the field increases, consistent with qualitative variation seen in Fig. 2(b). In specific, at low field there is a competition between NNH and ES-VRH, with the prefactor ρ_0 accounts for the combined amplitude of the two contributions. At high field ρ_0 becomes large and tends to saturation, while the value of exponent α becomes zero, indicating that ES-VRH dominates. In this regime, ρ_0 represents the resistivity at high temperature. T_0 shown in Fig. 3(d) decreases with increasing magnetic field. T_0 is inversely proportional to the localization length ξ_{loc}[35]. We therefore find that the localization length ξ_{loc} in-

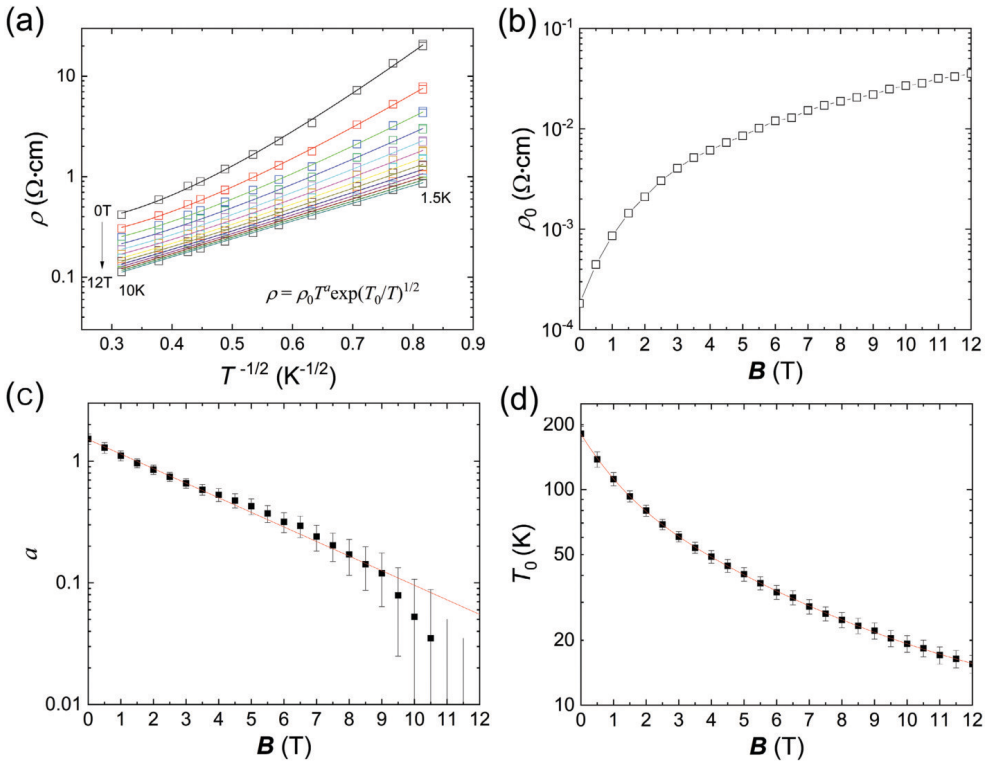

Fig. 3. (Color online) (a) Scaling of the resistivity versus $T^{-1/2}$ at different magnetic fields for lower temperatures. The curves are fits of Eq. (3), and (b), (c) and (d) show the field dependence of fitting parameters ρ_0, α and T_0. The red curve fits in (c) and in (d) have a decaying exponential form.

creases with magnetic field in the ES-VRH regime[27, 36].

Generally speaking, conductivity in the NNH and VRH regimes is given by[32, 33]

$$\rho^{-1} = \sigma = e^2 R_{ij}^2 \nu_{\rm ph} N(E_{\rm F}) \exp\left(-\frac{2R_{ij}}{\xi_{\rm loc}} - \frac{W_{ij}}{k_{\rm B}T}\right), \qquad (4)$$

where R_{ij} is the hopping distance between sites i and j, $\nu_{\rm ph}$ the phonon frequency, $N(E_{\rm F})$ the Fermi density of states, $\xi_{\rm loc}$ the carrier localization length, and W_{ij} the potential energy difference (effective hopping barrier) between hopping sites i and j. If non-VRH contributions co-exist with VRH, the temperature dependent term proportional to $\frac{W_{ij}}{k_{\rm B}T}$ can play a determining role in the MR. When $k_{\rm B}T$ is smaller than W_{ij}, the thermally activated carriers are no longer present to ensure conductivity. In this case, the temperature dependence of the resistivity relies on the variation of $\exp\left(-\frac{2R_{ij}}{\xi_{\rm loc}}\right)$, and the Eq. (4) evolves into Eq. (3). When $\xi_{\rm loc}$ increases with increasing field to a value that is much larger than the nearest-neighbor hopping distance, $\exp\left(-\frac{2R_{ij}}{\xi_{\rm loc}}\right)$ becomes dominant over $\exp\left(-\frac{W_{ij}}{k_{\rm B}T}\right)$ and we recover Eq. (2). This basic criterion was suggested by Mott and Davis[33] in the absence of interactions, but the same argument leads to Eq. (2), but with s = 1/2 when a Coulomb gap is present[4, 28].

In Fig. 4, we are able to rule out some possibility by examining the field dependent resistivity at higher between 10 and 30 K ($T > T_s$) where NNH hopping is found to be dominant. Fig. 4(a) clearly shows that ρ varies following Eq. (1) in this temperature range. A fit using Eq. (1) yields $T_1 \sim W_{ij}$ and $\rho_1 \sim R_{ij}^{-2}\exp\left(\frac{2R_{ij}}{\xi_{\rm loc}}\right)$. T_1 is nearly constant versus magnetic field, while ρ_1 decreases by more than order of magnitude. The fact that T_1 is constant in the NNH regime can be used to rule out the presence of a field dependent W_{ij}. From this we conclude that, the increasing localization length $\xi_{\rm loc}$ as the magnetic field increases[27, 36] can explain the observed CNMR even in the NNH regime.

4. Discussion and remarks

At low temperatures the conductivity of $Ga_{1-x}Mn_xAs_{1-y}P_y$ films with high phosphorus concentration y is determined by hopping. In this regime, two different hopping mechanisms can determine the conductivity: NNH and ES-VRH. When a high magnetic field is applied (B > 7 T), at temperatures $T < T_s$ ES-VRH becomes the dominant hopping mechanism in samples studied in this paper. In both regimes, the CNMR is driven by the field dependence of the localization length, whose impact on ρ is exponential. In Fig. 3(d), we have shown that T_0 decays with increasing field following a decay function $f(B)$ that drives the CNMR as:

$$\rho \sim \exp\left(\frac{f(B)}{T}\right)^{1/2}. \qquad (5)$$

T_0 is inversely proportional to the localization length $\xi_{\rm loc}$ for ES-VRH[6]. The physical meaning of the localization length $\xi_{\rm loc}$ is defined by $\psi_{\rm E}(R) \sim {\rm e}^{-R/\xi_{\rm loc}}$, the envelope function of the Anderson localized state with energy E. It is known that $\xi_{\rm loc}(E_{\rm f}) \propto (|E_{\rm m} - E_{\rm f}|)^{-\upsilon}$, where $E_{\rm m}$ is the mobility edge, $E_{\rm f}$ the Fermi level and the exponent υ has a value close to 1[37]. The behavior of T_0 thus indicates that the mobility edge becomes field dependent, which drives the CNMR.

In insulating ferromagnetic $Ga_{1-x}Mn_xAs_{1-y}P_y$ films the random distribution of P atoms has two significant effects. It leads to a spatial randomness of the valence band edge and to local variations in magnetic anisotropy which is driven by local lattice strain. A strong magnetic field suppresses local

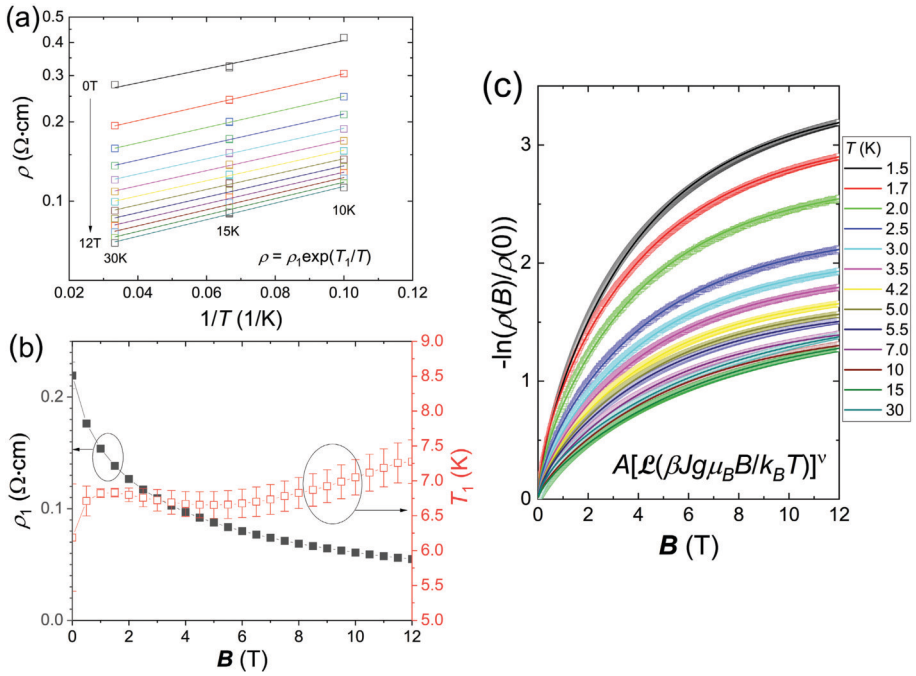

Fig. 4. (Color online) (a) Scaling of the resistivity versus $1/T$ at different magnetic fields at higher temperatures. The curves are fits to Eq. (1). (b) Magnetic field dependence of fitting parameters ρ_1 and T_1. (c) Logarithm scale of the magnetoresistance versus magnetic field fitted with a Langevin function.

magnetic randomness, leading to a more uniform distribution of hopping sites, thus reducing the value of $|E_m - E_f|$[38]. The decay of $|E_m - E_f|$ will in this case follow a paramagnetic saturation which leads to $f(B) \sim e^{-B}$ as seen in Fig. 4(c), keeping in mind that the Langevin $\mathfrak{L}(x)$ and Brillouin functions approach their asymptote exponentially. Despite the magnetization saturating at low magnetic fields, this local randomness of the anisotropy of the magnetic moment can thus drive the CNMR. In Fig. 4(c), we show that the $\rho(B)/\rho(B = 0)$ follows indeed Eq. (6) with $f(B) = \mathfrak{L}(x)$ where $x = \beta J g \mu_B B/k_B T$. More details of this fit and its results are shown in Supplementary Material, its excellent agreement with the data confirming our hypothesis.

5. Conclusion

In conclusion, we have provided a consistent physical picture that explains the colossal negative MR observed in $Ga_{1-x}Mn_xAs_{1-y}P_y$ at low temperature and the increase in resistivity. These effects exist far away from the Curie temperature, in samples that retain a strong ferromagnetic interaction, despite their charge carriers entering into a strong localization regime. Magnetic field thus lowers resistance as it suppresses localization. A similar behavior has been ascribed to an increasing localization length in magnetic II–VI semiconductors, but for samples with a much lower charge density in the quantum limit[39–41]. However, in $Ga_{1-x}Mn_xAs_{1-y}P_y$, we find a metal insulator transition occurring for samples with high charge density in the presence of a Coulomb gap and ferromagnetism. A deeper theoretical understanding of localization physics[24, 42] is needed in this regime.

Acknowledgements

We thank Jacek Kossut and Boldizsar Janko for valuable discussions. This work was supported by the National Science Foundation Grant No. DMR 1905277.

Appendix A. Supplementary materials

Supplementary materials to this article can be found online at https://doi.org/10.1088/1674-4926/43/11/112502.

References

[1] Thouless D J. Electrons in disordered systems and the theory of localization. Phys Rep, 1974, 13, 93
[2] Sondhi S L, Girvin S M, Carini J P, et al. Continuous quantum phase transitions. Rev Mod Phys, 1997, 69, 315
[3] Mott N F. Conduction in non-crystalline materials. Philos Mag, 1969, 19, 835
[4] Efros A L, Shklovskii B I. Electronic properties of doped semiconductors. Berlin: Springer, 1984
[5] Mott N F. Conduction in glasses containing transition metal ions. J Non Cryst Solids, 1968, 1, 1
[6] Efros A L, Shklovskii B I. Coulomb gap and low temperature conductivity of disordered systems. J Phys C, 1975, 8, L49
[7] Zhang Y Z, Dai O, Levy M, et al. Probind the coulomb gap in insulating n-type CdSe. Phys Rev Lett, 1990, 64, 2687
[8] Aharony A, Zhang Y, Sarachik M P. Universal crossover in variable range hopping with Coulomb interactions. Phys Rev Lett, 1992, 68, 3900
[9] Viret M, Ranno L, Coey J M D. Colossal magnetoresistance of the variable range hopping regime in the manganites. J Appl Phys, 1997, 81, 4964
[10] Masarrat A, Bhogra A, Meena R, et al. Enhancement of the thermoelectric properties and transition of conduction mechanism from nearest neighbor to variable range hopping of Ni-doped $CoSb_3$. J Electron Mater, 2022, 51, 3350
[11] Zhang L J, King I, Nasyedkin K, et al. Coherent hopping transport and giant negative magnetoresistance in epitaxial $CsSnBr_3$. ACS Appl Electron Mater, 2021, 3, 2948
[12] Xue J H, Huang S Y, Wang J Y, et al. Mott variable-range hopping transport in a MoS_2 nanoflake. RSC Adv, 2019, 9, 17885
[13] Rimal G, Tang J K. Magnetic hard gap due to bound magnetic polarons in the localized regime. Sci Rep, 2017, 7, 42224

[14] Joung D, Khondaker S I. Efros-Shklovskii variable range hopping in reduced graphene oxide sheets of varying carbon sp2 fraction. Phys Rev B, 2012, 86, 235423
[15] Punia R, Kundu R S, Murugavel S, et al. Hopping conduction in bismuth modified zinc vanadate glasses: An applicability of Mott's model. J Appl Phys, 2012, 112, 113716
[16] Iye Y, Oiwa A, Endo A, et al. Metal-insulator transition and magnetotransport in III-V compound diluted magnetic semiconductors. Mater Sci Eng B, 1999, 63, 88
[17] Dong S N, Riney L, Liu X Y, et al. Carrier localization in quaternary $Ga_{1-x}Mn_xAs_{1-y}P_y$ ferromagnetic semiconductor films. Phys Rev Mater, 2021, 5, 014402
[18] Liu X Y, Dong S N, Riney L, et al. Crossover behavior of the anomalous Hall effect in $Ga_{1-x}Mn_xAs_{1-y}P_y$ across the metal-insulator transition. Phys Rev B, 2021, 103, 214437
[19] Lee H, Chang J, Chongthanaphisut P, et al. Magnetic anisotropy of quaternary GaMnAsP ferromagnetic semiconductor. AIP Adv, 2017, 7, 055809
[20] Li X, Liu X Y, Dong S N, et al. Dependence of ferromagnetic properties on phosphorus concentration in $Ga_{1-x}Mn_xAs_{1-y}P_y$. J Vac Sci Technol B, 2018, 36, 02D104
[21] Takeda Y, Ohya S, Pham N H, et al. Direct observation of the magnetic ordering process in the ferromagnetic semiconductor $Ga_{1-x}Mn_xAs$ via soft X-ray magnetic circular dichroism. J Appl Phys, 2020, 128, 213902
[22] Onoda S, Sugimoto N, Nagaosa N. Quantum transport theory of anomalous electric, thermoelectric, and thermal Hall effects in ferromagnets. Phys Rev B, 2008, 77, 165103
[23] Wagner P, Gordon I, Trappeniers L, et al. Spin dependent hopping and colossal negative magnetoresistance in epitaxial $Nd_{0.52}Sr_{0.48}MnO_3$ films in fields up to 50 T. Phys Rev Lett, 1998, 81, 3980
[24] Zaránd G, Moca C P, Jankó B. Scaling theory of magnetoresistance in disordered local moment ferromagnets. Phys Rev Lett, 2005, 94, 247202
[25] Oiwa A, Katsumoto S, Endo A, et al. Nonmetal-metal-nonmetal transition and large negative magnetoresistance in (Ga, Mn)As/GaAs. Solid State Commun, 1997, 103, 209
[26] Yuan Y, Xu C, Hübner R, et al. Interplay between localization and magnetism in (Ga, Mn)As and (In, Mn)As. Phys Rev Mater, 2017, 1, 054401
[27] Yakimov A I, Wright T, Adkins C J, et al. Magnetic correlations on the insulating side of the metal-insulator transition in amorphous $Si_{1-x}Mn_x$. Phys Rev B, 1995, 51, 16549
[28] Yildiz A, Serin N, Serin T, et al. Crossover from nearest-neighbor hopping conduction to Efros–Shklovskii variable-range hopping conduction in hydrogenated amorphous silicon films. Jpn J Appl Phys, 2009, 48, 111203
[29] Dlimi S, El kaaouachi A, Limouny L, et al. A crossover from Efros-Shklovskii hopping to activated transport in a GaAs two-dimensional hole system at low temperatures. J Semicond, 2021, 42, 052001
[30] Street R A. Hydrogenated amorphous silicon. Cambridge University Press, 1991
[31] Miller A, Abrahams E. Impurity conduction at low concentrations. Phys Rev, 1960, 120, 745
[32] Mott N F. Conduction in non-crystalline materials. Oxford: Clarendon Press, 1987
[33] Mott N F, Davis E A. Electronic processes in non-crystalline materials. Oxford: Clarendon Press, 1971
[34] van Keuls F W, Hu X L, Jiang H W, et al. Screening of the Coulomb interaction in two-dimensional variable-range hopping. Phys Rev B, 1997, 56, 1161
[35] Adkins C J. Conduction in granular metals-variable-range hopping in a Coulomb gap? J Phys: Condens Matter, 1989, 1, 1253
[36] Penney T, von Molnár S, et al. Low-temperature transport properties of $Cd_{0.91}Mn_{0.09}Te$: In and evidence for a magnetic hard gap in the density of states. Phys Rev Lett, 1992, 69, 1800
[37] Evers F, Mirlin A D. Anderson transitions. Rev Modern Phys, 2008, 80, 63
[38] Egli D, Fröhlich J, Ott H R. Anderson localization triggered by spin disorder – with an application to $Eu_xCa_{1-x}B_6$. J Statist Phys, 2011, 143, 970
[39] Wojtowicz T, Mycielski A. Magnetic field induced nonmetal-metal transition in the open-gap $Hg_{1-x}Mn_xTe$. Phys B+C, 1983, 117, 476
[40] Wojtowicz T, Gawron T R, Robert J L, et al. Hopping conductions studies of p-$Hg_{1-x}Mn_xTe$ in high magnetic fields: Unusual anisotropy of resistivity. J Cryst Growth, 1985, 72, 385
[41] Mycielski J. Shallow acceptors in DMS: Splitting, boil-off, giant negative magnetoresistance. Semiconductors and Semimetals, 1988, 25, 311
[42] Moca C P, Sheu B L, Samarth N, et al. Scaling theory of magnetoresistance and carrier localization in $Ga_{1-x}Mn_xAs$. Phys Rev Lett, 2009, 102, 137203

Xinyu Liu is a research associate professor in the Department of Physics and Astronomy at University of Notre Dame. His research is centered on studies of spin-based phenomenon in quantum materials. He is a specialist on developing the integrated nanostructures based on semiconductors, superconductor, and magnetic materials using MBE.